

GENERATION OF CELL-LIKE IMAGES WITH VARIABLE PATTERN SIZE FROM RGB-D IMAGES

TORU HIRAOKA

Department of Information Systems
University of Nagasaki
1-1-1, Manabino, Nagayo-chou, Nishisonogi-gun, Nagasaki-ken 851-2195, Japan
hiraoka@sun.ac.jp

Received November 2021; accepted January 2022

ABSTRACT. *A non-photorealistic rendering method has been proposed to generate cell-like images from photographic images using an inverse iris filter and distance from the edges of the photographic images. In this study, we propose a method to change the size of cell-like patterns according to the depth by using RGB-D images, and to generate the cell-like patterns in white and black areas where the cell-like patterns were less likely to occur in the conventional method. To verify the effectiveness of the proposed method, experiments were conducted to visually confirm the cell-like images generated by changing the parameters in the proposed method.*

Keywords: Non-photorealistic rendering, Cell pattern, Cell-like image, RGB-D image, Pattern size, Inverse iris filter

1. **Introduction.** Non-photorealistic rendering is one of computer graphics [1, 2, 3] that creates images with artificial enhancements such as illustrations and painting [4, 5, 6, 7, 8, 9]. A method for generating cell-like images from photographic images has been proposed for non-photorealistic rendering [10, 11, 12]. The cell-like images are expressed by superimposing cell-like patterns that imitate the cell membrane and cell nucleus on the photographic images, and the cell-like patterns locally change in accordance with the edges and shades of the photographic images. The generation of the cell-like images enables users to convert the photographic images captured using a smartphone into the cell-like images, and upload them to a social networking service. For the generation of the cell-like images, a conventional method proposed in [10] used an inverse iris filter, [11] used the inverse iris filter and photographic images that synthesize sine and cosine waves, and [12] used the inverse iris filter and Euclidean distance from the edges. The conventional method [11] extended the conventional method [10] to emphasize and align cell patterns in cell-like images. The conventional method [12] expressed the cell membrane and cell nucleus of the cell-like patterns more clearly than the conventional method [10], and generated the cell-like patterns along the edges. However, the size of the cell-like patterns by the conventional methods was constant, and the cell-like patterns were less likely to occur in white and black areas of the photographic images. By partially changing the size of the cell-like patterns, the expression of the cell-like images can be expanded, and by being represented the cell-like patterns in the entire image, the visual effect of the cell-like images can be improved.

In recent years, a smartphone with a stereo camera has appeared, and RGB-D images with RGB values and depth have become familiar. Therefore, we propose a method to change the size of the cell-like patterns according to the depth by using the RGB-D images instead of the photographic images in the conventional method [12]. In addition, we propose a method to generate the cell-like patterns in the white and black areas by

converting the brightness of the photographic images as a pre-processing of the conventional method [12]. To verify the effectiveness of the proposed method, an experiment was conducted to visually compare cell-like images of the proposed method with cell-like images of the conventional method. Furthermore, an experiment was conducted to visually confirm the cell-like images by changing the values of newly added parameters in the proposed method.

This paper is organized as follows: the second section describes the proposed method to generate cell-like images from RGB-D images, the third section shows experimental results and reveals the effectiveness of the proposed method, and the conclusion of this paper is given in the fourth section.

2. Proposed Method. The proposed method was implemented in three steps: 1) create distance-transformed images by calculating Euclidean distance from the edges of the RGB values of the RGB-D images using the depth; 2) convert the RGB values; 3) generate cell-like images from the distance-transformed images and the converted RGB values using the inverse iris filter. The flow chart of the proposed method is shown in Figure 1.

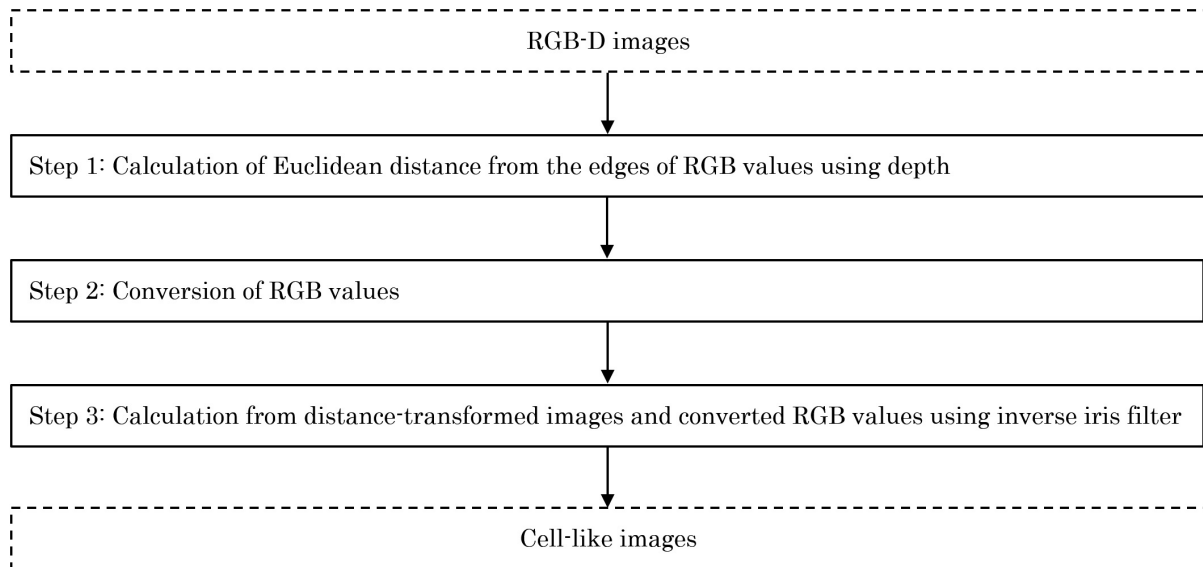


FIGURE 1. Flow chart of the proposed method

The detailed procedure of the proposed method is as follows.

Step 0: The input pixel values (R, G, B) and the depth for spatial coordinates (i, j) of an RGB-D image are defined as $f_{R,i,j}$, $f_{G,i,j}$, $f_{B,i,j}$, and $f_{D,i,j}$, respectively. The pixel values $f_{R,i,j}$, $f_{G,i,j}$, and $f_{B,i,j}$ have value of U gradation from 0 to $U - 1$. The depths $f_{D,i,j}$ are stored in centimeters and the unit of depths $f_{D,i,j}$ is meters.

Step 1: At each pixel, the parameters $w_{i,j}$ that determine the size of the cell-like patterns are calculated using the depth $f_{D,i,j}$ in the following equation:

$$w_{i,j} = w_{\max} - \frac{(w_{\max} - w_{\min})(f_{D,i,j} - f_{D,\min})}{f_{D,\max} - f_{D,\min}} \quad (1)$$

where $f_{D,\min}$ and $f_{D,\max}$ are respectively the minimum and maximum values in the depth $f_{D,i,j}$, and w_{\min} and w_{\max} are respectively the minimum and maximum window sizes set by the user. The smaller the values of the depth $f_{D,i,j}$, the larger the size of the cell-like patterns.

Gray-scale pixel values $f_{i,j}$ are calculated in the following equation:

$$f_{i,j} = \frac{f_{R,i,j} + f_{G,i,j} + f_{B,i,j}}{3} \quad (2)$$

Edges are extracted from the gray-scale image using EDISON [13] that is a feature extraction tool that integrates edge detection and image segmentation. The shortest Euclidean distances $d_{1,i,j}$ from the edge pixels are calculated at each pixel.

If the Euclidean distances $d_{1,i,j}$ are within $mw_{i,j} + w_{i,j}/2 \pm 0.5$ ($m = 0, 1, 2, \dots$), the Euclidean distances $d_{2,i,j}$ are set to 0. Otherwise, the Euclidean distances $d_{2,i,j}$ are set to ∞ . When the positions where the Euclidean distances $d_{2,i,j}$ are 0 are expressed on the image, it becomes lines of the interval $w_{i,j}$ along the edges.

Scanned from the upper left to the lower right of the image, and in the case that the Euclidean distances $d_{2,i,j}$ are 0 at the target pixel (i, j) , the Euclidean distances $d_{2,k,l}$ in the range where the Euclidean distance from the target pixel (i, j) is smaller than $w_{i,j}$ are updated to ∞ , where the pixels (k, l) are pixels when the Euclidean distance from the target pixel (i, j) is smaller than $w_{i,j}$, and the Euclidean distance $d_{2,i,j}$ of the target pixel (i, j) is not updated. When the positions where the Euclidean distances $d_{2,i,j}$ are 0 are expressed on the image, it becomes dotted lines with the spacing $w_{i,j}$.

Scanned from the upper left to the lower right of the image, and in the case that the Euclidean distances $d_{2,i,j}$ are ∞ at the target pixel (i, j) , the Euclidean distance $d_{2,i,j}$ of the target pixel (i, j) is updated to 0 if there is no pixel where the Euclidean distances $d_{2,k,l}$ are 0 in the range where the Euclidean distance from the target pixel (i, j) is smaller than $w_{i,j}$. In all pixels (i, j) , there are pixels that the Euclidean distances $d_{2,k,l}$ are 0 within the radius $w_{i,j}$.

The shortest Euclidean distances $d_{i,j}$ from the pixels that the Euclidean distances $d_{2,k,l}$ are 0 are calculated at each pixel. An image composed of the shortest Euclidean distances $d_{i,j}$ is called a distance-transformed image.

Step 2: The pixel values after converting the pixel values $f_{R,i,j}$, $f_{G,i,j}$, and $f_{B,i,j}$ are respectively defined as $g_{R,i,j}$, $g_{G,i,j}$, and $g_{B,i,j}$. If $f_{R,i,j} < b_1 \wedge f_{G,i,j} < b_1 \wedge f_{B,i,j} < b_1$ where b_1 is a positive constant set by the user, then $g_{R,i,j}$, $g_{G,i,j}$, and $g_{B,i,j}$ are respectively calculated in the following equations:

$$g_{R,i,j} = \frac{b_1 (f_{R,i,j} + 1)}{f_{1,i,j} + 1} \tag{3}$$

$$g_{G,i,j} = \frac{b_1 (f_{G,i,j} + 1)}{f_{1,i,j} + 1} \tag{4}$$

$$g_{B,i,j} = \frac{b_1 (f_{B,i,j} + 1)}{f_{1,i,j} + 1} \tag{5}$$

$$f_{1,i,j} = \max \{f_{R,i,j}, f_{G,i,j}, f_{B,i,j}\} \tag{6}$$

If $f_{R,i,j} > U - b_2 - 1 \wedge f_{G,i,j} > U - b_2 - 1 \wedge f_{B,i,j} > U - b_2 - 1$ where b_2 is a positive constant set by the user, then $g_{R,i,j}$, $g_{G,i,j}$, and $g_{B,i,j}$ are respectively calculated in the following equations:

$$g_{R,i,j} = \frac{(U - b_2 - 1) (f_{R,i,j} + 1)}{f_{2,i,j} + 1} \tag{7}$$

$$g_{G,i,j} = \frac{(U - b_2 - 1) (f_{G,i,j} + 1)}{f_{2,i,j} + 1} \tag{8}$$

$$g_{B,i,j} = \frac{(U - b_2 - 1) (f_{B,i,j} + 1)}{f_{2,i,j} + 1} \tag{9}$$

$$f_{2,i,j} = \min \{f_{R,i,j}, f_{G,i,j}, f_{B,i,j}\} \tag{10}$$

Otherwise, $g_{R,i,j}$, $g_{G,i,j}$, and $g_{B,i,j}$ are the following equations:

$$g_{R,i,j} = f_{R,i,j} \tag{11}$$

$$g_{G,i,j} = f_{G,i,j} \tag{12}$$

$$g_{B,i,j} = f_{B,i,j} \quad (13)$$

The above conversion makes it possible to generate the cell-like patterns in the white and black areas.

Step 3: The output pixel values after processing with an iris filter [14] on $d_{i,j}$ are defined as $C_{i,j}$. The iris filter is executed with the $2r + 1$ peripheral pixels (k, l) in the window of size r . Angles $\theta_{i,j,k,l}$ between a vector $(i - k, j - l)$ from the peripheral pixels (k, l) to the target pixel (i, j) and a vector $((d_{k+2,l+2} + d_{k+2,l+1} + d_{k+2,l} + d_{k+2,l-1} + d_{k+2,l-2}) - (d_{k-2,l+2} + d_{k-2,l+1} + d_{k-2,l} + d_{k-2,l-1} + d_{k-2,l-2}), (d_{k+2,l+2} + d_{k+1,l+2} + d_{k,l+2} + d_{k-1,l+2} + d_{k-2,l+2}) - (d_{k+2,l-2} + d_{k+1,l-2} + d_{k,l-2} + d_{k-1,l-2} + d_{k-2,l-2}))$ are computed. The convergence indices $c_{i,j}$ of the target pixel (i, j) are calculated as the following equation:

$$c_{i,j} = \frac{1}{2r + 1} \left| \sum_{k=i-r}^{i+r} \sum_{l=j-r}^{j+r} \cos \theta_{i,j,k,l} \right| \quad (14)$$

The minimum and maximum values of $c_{i,j}$ are defined as c_{\min} and c_{\max} , respectively. The convergence indices $c_{i,j}$ are converted to $C_{i,j}$ in the following equation:

$$C_{i,j} = 255 \left(\frac{c_{i,j} - c_{\min}}{c_{\max} - c_{\min}} \right) \quad (15)$$

Pixel values $h_{R,i,j}$, $h_{G,i,j}$ and $h_{B,i,j}$ are computed by using an inverse filter [15] in the following equations:

$$h_{R,i,j} = a (f_{i,j} - C_{i,j}) + g_{R,i,j} \quad (16)$$

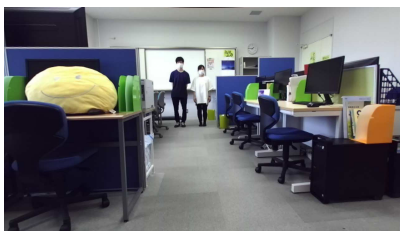
$$h_{G,i,j} = a (f_{i,j} - C_{i,j}) + g_{G,i,j} \quad (17)$$

$$h_{B,i,j} = a (f_{i,j} - C_{i,j}) + g_{B,i,j} \quad (18)$$

where a is positive constant. If $h_{R,i,j}$, $h_{G,i,j}$ and $h_{B,i,j}$ are less than 0, then these values must be set to 0, respectively. If $h_{R,i,j}$, $h_{G,i,j}$ and $h_{B,i,j}$ are greater than $U - 1$, then these values must be set to $U - 1$, respectively. The image composed of the pixel values $h_{R,i,j}$, $h_{G,i,j}$ and $h_{B,i,j}$ is a cell-like image of the proposed method.

3. Experiments. An RGB-D image was obtained using ZED stereo camera. In the following experiments, the RGB-D image in Figure 2 was used: the left and right sides of Figure 2 are the RGB and depth images, respectively. In the depth image, a white area indicates a greater distance. The RGB-D image comprised $1280 * 720$ pixels and 256 gradations. Referring to [12], the values of the parameters r and a were set to 3 and 0.4, respectively.

A cell-like image generated by the conventional method [12] is shown in Figure 3. The size of the cell-like patterns was constant. The cell-patterns were blurred in the white areas, such as the white board in the center of the image, and were also blurred in the



(a) RGB image



(b) Depth image

FIGURE 2. RGB-D image

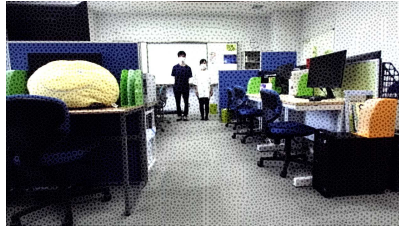
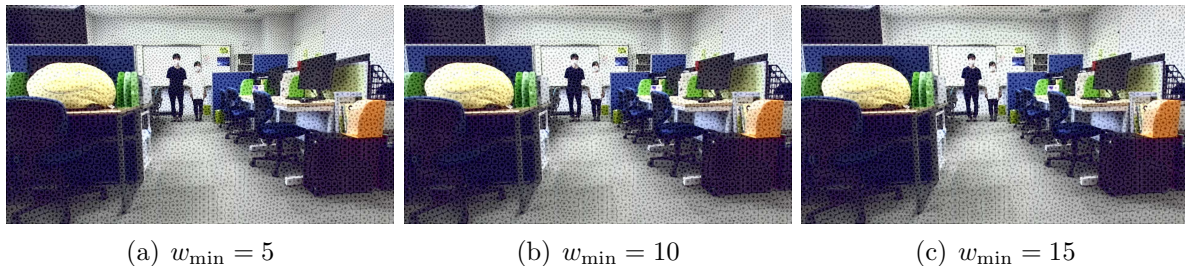


FIGURE 3. Cell-like images generated by the conventional method [12]

black areas, such as the shadows under the desk and computer in the lower right and lower left of the image.

In the following, the experiments were conducted with different values of the newly added parameters w_{\min} , w_{\max} , b_1 , and b_2 in the proposed method. And unless otherwise noted, the values of the parameters w_{\min} , w_{\max} , b_1 , and b_2 were set to 10, 20, 80, and 80, respectively.

First, cell-like images generated by changing the value of the parameter w_{\min} were visually confirmed. The value of w_{\min} was set to 5, 10, and 15. The experimental results are shown in Figure 4. A smaller value of w_{\min} resulted in a smaller representation of the distant cell-like patterns and an overall smaller representation of the cell-like patterns. In the conventional method [12], the size of the cell-like patterns could not be changed partially, but in the proposed method, the size of the cell-like patterns could be changed partially by changing the value of w_{\min} .



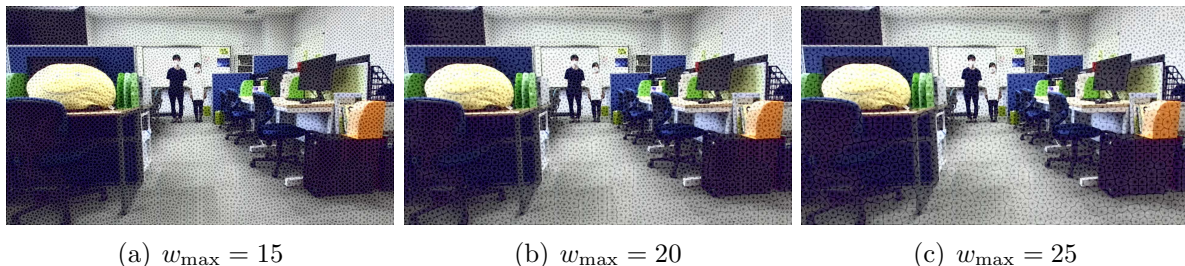
(a) $w_{\min} = 5$

(b) $w_{\min} = 10$

(c) $w_{\min} = 15$

FIGURE 4. Cell-like images generated by changing the value of w_{\min}

Next, cell-like images generated by changing the value of the parameter w_{\max} were visually confirmed. The value of w_{\max} was set to 15, 20, and 25. The experimental results are shown in Figure 5. A larger value of w_{\max} resulted in a larger representation of the nearby cell-like patterns and an overall large representation of the cell-like patterns. In the conventional method [12], the size of the cell-like patterns could not be changed partially, but in the proposed method, the size of the cell-like patterns could be changed partially by changing the value of w_{\max} .



(a) $w_{\max} = 15$

(b) $w_{\max} = 20$

(c) $w_{\max} = 25$

FIGURE 5. Cell-like images generated by changing the value of w_{\max}

Next, cell-like images generated by changing the value of the parameter b_1 were visually confirmed. The value of b_1 was set to 0, 40, and 80. The experimental results are shown in Figure 6. The larger value of b_1 , the clearer the cell-like patterns were represented in the black areas such as the shadows under the desk and computer in the lower right and lower left of the image. The proposed method could generate cell-like patterns in the black areas that could not be represented by the conventional method [12] by changing the value of b_1 .

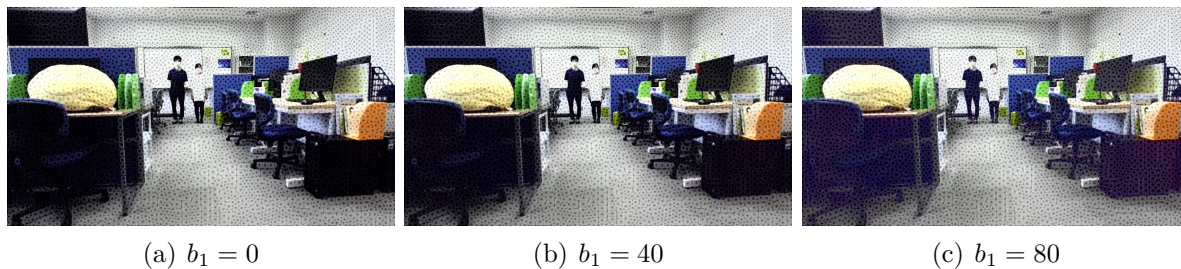


FIGURE 6. Cell-like images generated by changing the value of b_1

Finally, cell-like images generated by changing the value of the parameter b_2 were visually confirmed. The value of b_2 was set to 0, 40, and 80. The experimental results are shown in Figure 7. The larger value of b_2 , the clearer the cell-like patterns were represented in the white areas such as the white board in the center of the image. The proposed method could generate cell-like patterns in the white areas that could not be represented by the conventional method [12] by changing the value of b_2 .

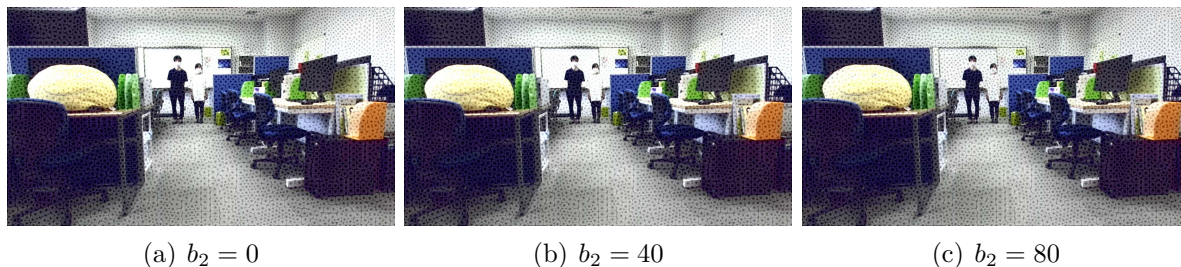


FIGURE 7. Cell-like images generated by changing the value of b_2

4. Conclusions. We proposed a non-photorealistic rendering method to generate cell-like images from RGB-D images using processing that extends the conventional method [12]. Experiments were conducted using an RGB-D image, and it was found that the proposed method can generate cell-like patterns in black and white areas that could not be generated by the conventional method [12]. In addition, it was found that the proposed method can change the size of the cell-like patterns partially according to the depth, which could not be changed by the conventional method [12].

A subject for future study is to expand the proposed method for application to RGB-D videos.

Acknowledgment. This work was supported by JSPS KAKENHI Grant Number JP19-K12664.

REFERENCES

- [1] H. Shen, Z. Zhang and Z. Shang, Fast global rendering in virtual reality via linear integral operators, *International Journal of Innovative Computing, Information and Control*, vol.15, no.1, pp.67-77, 2019.
- [2] L. Xue, X. Yi, Y.-C. Lin and J. W. Drukker, An approach of the product form design based on GRA-fuzzy logic model: A case study of train seats, *International Journal of Innovative Computing, Information and Control*, vol.15, no.1, pp.261-274, 2019.
- [3] F. Einabadi, J. Y. Guillemaut and A. Hilton, Deep neural models for illumination estimation and relighting: A survey, *Computer Graphics Forum*, vol.40, no.6, pp.315-331, 2021.
- [4] P. Haeblerli, Paint by numbers: Abstract image representations, *ACM SIGGRAPH Computer Graphics*, vol.24, no.4, pp.207-214, 1990.
- [5] J. Lansdown and S. Schofield, Expressive rendering: A review of nonphotorealistic techniques, *IEEE Computer Graphics and Applications*, vol.15, no.3, pp.29-37, 1995.
- [6] D. Martin, G. Arroyo, A. Rodriguez and T. Isenberg, A survey of digital stippling, *Computers & Graphics*, vol.67, pp.24-44, 2017.
- [7] W. Qian, D. Xu, J. Cao, Z. Guan and Y. Pu, Aesthetic art simulation for embroidery style, *Multimedia Tools and Applications*, vol.78, no.1, pp.995-1016, 2019.
- [8] T. Hiraoka, Generation of edge-enhancing labyrinth images using inverse filter and two improved Laplacian filters, *ICIC Express Letters*, vol.14, no.2, pp.121-127, 2020.
- [9] C. Xu, G. Sun and R. Liang, A survey of volume visualization techniques for feature enhancement, *Visual Informatics*, vol.5, no.3, pp.70-81, 2021.
- [10] T. Hiraoka, M. Hirota, K. Inoue and K. Urahama, Generating cell-like color images by inverse iris filter, *ICIC Express Letters*, vol.11, no.2, pp.399-404, 2017.
- [11] T. Hiraoka, A method for emphasizing and aligning patterns in cell-like images, *ICIC Express Letters*, vol.13, no.11, pp.1031-1037, 2019.
- [12] T. Hiraoka and K. Maeda, Generation of cell-like images using Euclidean distance from edge, *Journal of Robotics, Networking and Artificial Life*, vol.8, no.1, pp.14-17, 2021.
- [13] The Robust Image Understanding Laboratory at Rutgers University, *Edge Detection and Image Segmentation (EDISON) System*, <http://sid.ethz.ch/debian/orfeo-toolbox/OTB-3.20.0/Utilities/otbedison/help/doc/help.html>, 2002.
- [14] H. Kobatake and S. Hashimoto, Convergence index filter for vector fields, *IEEE Trans. Image Processing*, vol.8, no.8, pp.1029-1038, 1999.
- [15] Z. Yu and K. Urahama, Iterative method for inverse nonlinear image processing, *IEICE Trans. Fundamentals*, vol.E97-A, no.2, pp.719-721, 2014.